Neuron, Vol. 44, 769–778, December 2, 2004, Copyright ©2004 by Cell Press

Functional Recovery in a Primate Model of Parkinson's Disease following Motor Cortex Stimulation

Xavier Drouot,[1,3,4] Satoru Oshino,[1] Bechir Jarraya,[1] Laurent Besret,[1] Haruhiko Kishima,[1] Philippe Remy,[1,5] Julien Dauguet,[2] Jean Pascal Lefaucheur,[3,4] Frédéric Dollé,[2] Françoise Condé,[1] Michel Bottlaender,[2] Marc Peschanski,[3] Yves Kéravel,[6] Philippe Hantraye,[1,2] and Stéphane Palfi[1,6,*]

[1]URA CEA-CNRS 2210
[2]Isotopic Imaging
Biochemical and Pharmacological Unit
and Imagene Program
Service Hospitalier Frédéric Joliot
91401 Orsay
France
[3]INSERM/UPVM U 421
University Paris 12
94010 Créteil
France
[4]Service de Physiologie
[5]Service de Neurologie
[6]Service de Neurochirurgie
Henri Mondor Hospital
AP-HP
University Paris 12
94010 Créteil
France

Summary

A concept in Parkinson's disease postulates that motor cortex may pattern abnormal rhythmic activities in the basal ganglia, underlying the genesis of observed motor symptoms. We conducted a preclinical study of electrical interference in the primary motor cortex using a chronic MPTP primate model in which dopamine depletion was progressive and regularly documented using ^{18}F-DOPA positron tomography. High-frequency motor cortex stimulation significantly reduced akinesia and bradykinesia. This behavioral benefit was associated with an increased metabolic activity in the supplementary motor area as assessed with 18-F-deoxyglucose PET, a normalization of mean firing rate in the internal globus pallidus (GPi) and the subthalamic nucleus (STN), and a reduction of synchronized oscillatory neuronal activities in these two structures. Motor cortex stimulation is a simple and safe procedure to modulate subthalamo-pallido-cortical loop and alleviate parkinsonian symptoms without requiring deep brain stereotactic surgery.

Introduction

In Parkinson's disease (PD), the progressive degeneration of dopaminergic mesencephalic neurons results in a gradual motor impairment including akinesia, bradykinesia, rigidity, and tremor. These symptoms arise from complex dysfunctional rearrangements occurring in neural circuits responsible for motor activity that relay in the striatum. Pathological hyperactivity is also known to occur in the two major output regions of the striatum, the subthalamic nucleus (STN) and the internal globus pallidus (GPi; DeLong, 1990). Over the past 10 years, functional interference with these pathologically driven neuronal activities using low-voltage/high-frequency electrical stimulation delivered to either the STN or the GPi through stereotactically implanted intraparenchymal electrodes has demonstrated major therapeutic value (Krack et al., 1998; Limousin et al., 1998). However, the complexity of the procedure, which requires a skilled stereotactician neurosurgeon to locate the electrodes into narrow deep brain nuclei, and the documented risks of electrode misplacement currently restrict the use of high-frequency deep brain stimulation to a limited number of patients (Bejjani et al., 1999; Houeto et al., 2002).

In a search for an alternative target structure accessible to electrical stimulation with fewer technical constraints, we identified the primary motor cortex as a possible candidate. Indeed, parkinsonian symptoms have been associated with pathological synchronized oscillatory neuronal activities in various output regions of the basal ganglia and in the primary motor cortex (Goldberg et al., 2002; Wichmann and DeLong, 1999), and recent experimental findings point to a direct implication of the motor cortex in the patterning of these pathological rhythmic activities (Bevan et al., 2002; Magill et al., 2001). These observations and the fact that cortical stimulation would require a less invasive stereotactic approach with no intraparenchymal implantation prompted us to investigate whether direct functional circuit interference in the motor cortex would achieve therapeutic efficacy in a nonhuman primate model of PD.

Results

The Nonhuman Primate Model of PD

As previously described (Poyot et al., 2001), the 52 week long 1-methyl-4-phenyl-1,2,3,6-tetrahydropyridine (MPTP) treatment induced in all baboons a progressive worsening of parkinsonian symptoms including a decrease of movement initiation (akinesia) and a decrease of movement velocities (bradykinesia) when the stimulator was kept in the "OFF" position (Figures 1A–1C). This gradual motor impairment was associated with a progressive bilateral decrease in ^{18}F-DOPA striatal uptake in all baboons and severe nigrostriatal degeneration (Figures 1D and 1G). Based on clinical studies showing that symptom onset occurs when ^{18}F-DOPA uptake has decreased to 60% of control values in PD patients (Ribeiro et al., 2002), three different stages of ^{18}F-DOPA depletion were defined in MPTP baboons (mild, moderate, and severe) corresponding to ^{18}F-DOPA uptake values above 60% of control uptake (mild depletion), between 59% and 40% (moderate depletion), and below 39% (severe depletion), respectively. These stages of striatal dopa-

*Correspondence: stephane.palfi@hmn.ap-hop-paris.fr

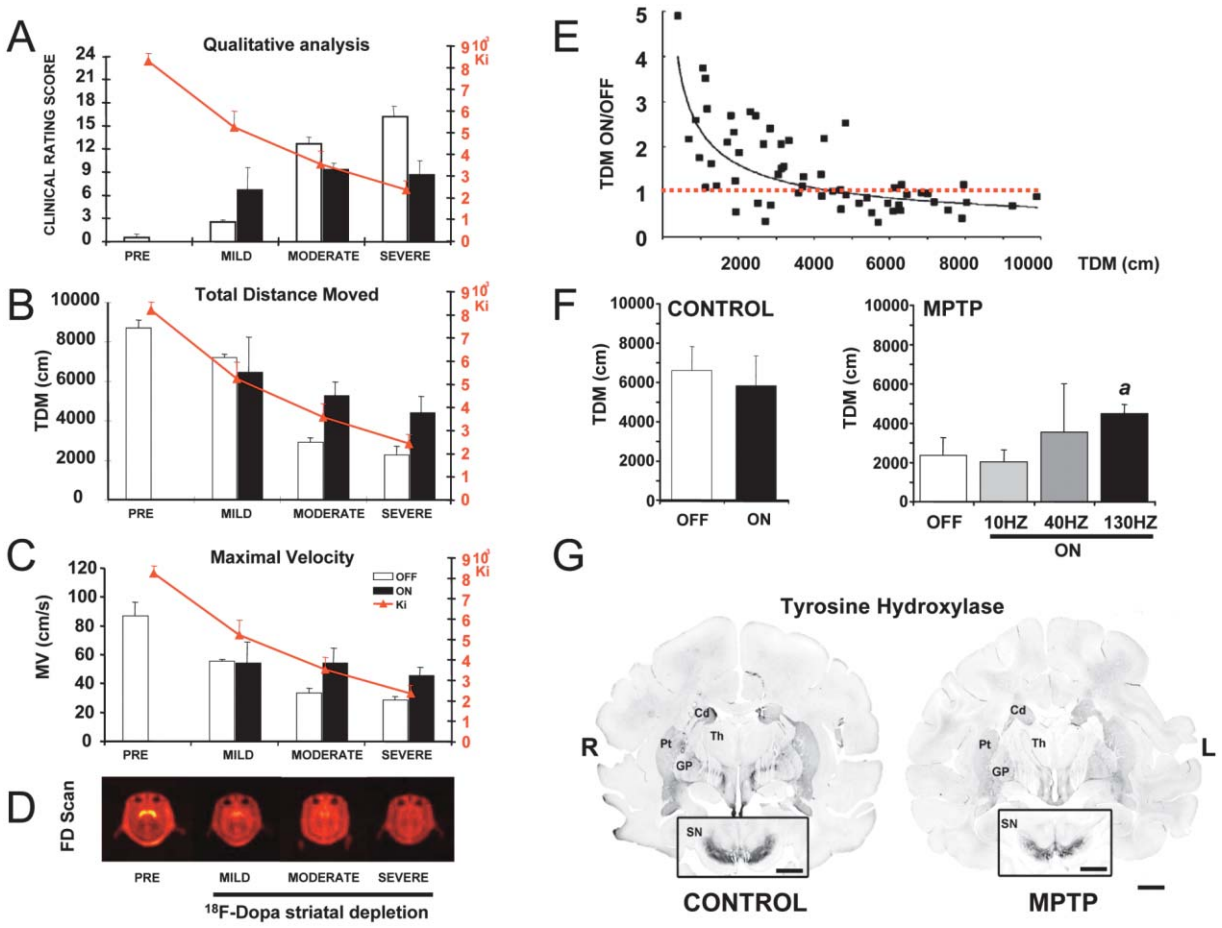

Figure 1. MCS Reduces Parkinsonian Symptoms in Primates Displaying Moderate and Severe ^{18}F-DOPA Striatal Uptake Depletions

(A) Histogram illustrating the progression of parkinsonian symptoms (increase in clinical rating score OFF; open bars; one way ANOVA analysis; Kruskall-Wallis [KW], $p < 0.05$) and the associated progressive decrease of ^{18}F-DOPA striatal uptake (Ki value, red line) during the 52 weeks chronic MPTP treatment. Note the significant decrease in clinical rating score induced by MCS (ON, solid bars), only observed in primates with moderate or severe ^{18}F-DOPA striatal depletions (WSR, $p < 0.05$).

(B) Histogram displaying the progressive increase in akinesia (reduction in TDM) observed during the chronic MPTP intoxication. MCS specifically ameliorated akinesia in animals only displaying moderate and severe ^{18}F-DOPA striatal depletions and not in animals with mild ^{18}F-DOPA striatal depletions (solid bars).

(C) Histogram displaying the progressive decrease in movement velocity (reduction in MV) during the chronic MPTP intoxication. Again, MCS selectively ameliorated bradykinesia in animals with moderate and severe ^{18}F-DOPA striatal depletion (solid bars).

(D) Serial ^{18}F-DOPA-PET scans performed on a regular basis during the entire MPTP intoxication and depicting the progressive reduction in ^{18}F-DOPA striatal uptake in the chronically MPTP-treated animals, compared to controls.

(E) Scatter plots illustrating the significant correlation observed between the ON/OFF TDM ratio (an index of MCS's therapeutic effect) and the degree of akinesia represented by TDM values recorded in the parkinsonian animals under OFF conditions (Spearman correlation test, $\rho = -0.65$; $p < 0.0001$). Note that behavioral recovery was more prominent in parkinsonian animals displaying the most severe stages of akinesia (lowest TDM OFF values) and that MCS had no effect either in control animals or the mildly affected MPTP baboons.

(F) (Left panel) Histogram demonstrating the lack of significant difference in TDM between ON and OFF in nonlesioned control animals ($p > 0.5$, WSR). (Right panel) Histogram of TDM in MPTP-lesioned animal as a function of the MCS frequency. Only high-frequency MCS (130 Hz) significantly improved animal performance as compared to OFF condition ($^{a}p < 0.05$, WSR).

(G) Low-power photomicrographs of brain sections from one control (left) and one MPTP-treated baboon (right), immunoreacted for tyrosine hydrolysase (TH) detection. Compared to controls, brain sections of MPTP animals displayed a severe decrease of TH-ir fibers bilaterally in the caudate and putamen and a loss of TH-ir neurons in the substantia nigra pars compacta and ventral tegmental area. As reported previously in chronic MPTP-treated primates, depletion of TH-ir fibers was more prominent in the putamen compared to the caudate nucleus, a neuropathological situation comparable to PD. Cd, caudate nucleus; Pt, putamen; SN, substantia nigra; Th, thalamus; GP, globus pallidus. Scale bar, 5 mm.

minergic deficiency corresponded to nondisabled (clinical rating score <4), moderately disabled (between 4 and 15), and severely disabled animals (above 15) (Figure 1A).

Efficacy of Motor Cortex Stimulation

Turning the stimulator in the "ON" position for a 30 min long train (monopolar; two cathodal contacts; 160 μs wide; 2.5 ± 0.4 V pulses; 130 Hz) did not affect motor

behavior in control animals and nondisabled animals with mild ^{18}F-DOPA depletion (Figures 1A and 1F). In contrast, motor symptoms were significantly reduced by motor cortical stimulation (MCS) in moderately and severely disabled animals displaying either moderate or severe ^{18}F-DOPA depletion. At these stages of dopamine depletion, MCS induced a significant improvement of akinesia and bradykinesia that was illustrated by a significant decrease in the clinical rating score (15 $\pm$ 1 [OFF] versus 9 $\pm$ 1 [ON]; Wilcoxon sign rank test [WSR], $p < 0.05$) (Figure 1A). Further behavioral analysis of the time course of motor improvement during the 30 min stimulating session showed that MPTP animals displayed a detectable improvement of behavioral symptoms following several minutes after turning ON MCS. Moreover, while MCS did not modify postural symptoms or balance impairments, the behavioral benefit was especially marked for items related to akinesia, bradykinesia, walking initiation (13 $\pm$ 2 [OFF] versus 26 $\pm$ 5 [ON]; WSR, $p < 0.05$), and climbing behavior (8 $\pm$ 2 [OFF] versus 16 $\pm$ 4 [ON]; WSR, $p < 0.05$).

Over the first 4 months of neurotoxic treatment, quantitative video-movement analysis, which provides an objective assessment of akinesia (total distance moved [TDM]) or bradykinesia (maximal velocity [MV]) showed a progressive decrease of TDM and MV values in OFF condition, which remained stable below 50% of initial control values. Compared to the OFF condition, MCS produced a significant 50% increase in TDM and MV in moderately and severely disabled animals with moderate or severe ^{18}F-DOPA depletion (2590 $\pm$ 260 cm [TDM OFF] versus 4840 $\pm$ 377 cm [ON]; WSR, $p < 0.05$; 31 $\pm$ 2 cm/s [MV OFF] versus 50 $\pm$ 6 cm/s [ON]; WSR, $p < 0.05$) but not in nondisabled or nonlesioned control animals (6683 $\pm$ 1223 [TDM OFF] versus 5899 $\pm$ 1541 [ON]; WSR, $p > 0.4$), confirming the clinical observations (Figures 1B, 1C, and 1F). To assess the relationship between behavioral benefit produced by MCS and the degree of hypokinesia, all video sessions performed in MPTP-treated animals were gathered together, regardless of the stage of parkinsonism. A beneficial effect of MCS on akinesia (ON/OFF TDM ratio >1) was correlated with the degree of motor impairment, indicating that the behavioral recovery was more prominent in animals displaying the most severe stage of akinesia and ^{18}F-DOPA depletion (Figure 1E).

The behavioral benefit was also associated with high-frequency stimulation (130 Hz), as MPTP animals did not display any significant motor improvement at either low (10 Hz; 2369 $\pm$ 913 [OFF] versus 2039 $\pm$ 599 [ON]; WSR, $p > 0.5$) or intermediate frequencies of stimulation (40 Hz; 2369 $\pm$ 913 [OFF] versus 4067 $\pm$ 3133 [ON]; WSR, $p > 0.5$) (Figure 1F). No adverse side effects such as seizures, motor deficit, and abnormal movements were detected with high-frequency MCS in any animals at any stage of ^{18}F-DOPA depletion.

Positron Emission Tomography Scan Changes

To gain insights on the mechanisms of action of MCS, we conducted a series of positron emission tomography (PET) imaging studies using either ^{18}F-DOPA or ^{18}F-Deoxyglucose (FDG) as radiotracers. PET scans that were performed in normal and severely disabled MPTP baboons did not reveal any significant changes in striatal uptake of ^{18}F-DOPA between ON and OFF conditions, arguing against a direct modulatory effect of MCS on nigrostriatal dopaminergic terminals. In contrast, FDG PET imaging studies in baboons with severe ^{18}F-DOPA depletion showed that MCS could activate cerebral regions implicated in cortical motor control loops. Thus, MCS selectively increased regional metabolic rate of glucose consumption between ON and OFF states, in the ipsilateral mesial premotor cortex, which comprises the supplementary motor area (SMA) and the pars dorsalis of the cingulate motor cortex (Figure 2) (Supplemental Movie S1 at http://www.neuron.org/cgi/content/full/44/5/769/DC1/). In contrast, SPM analysis did not identify any reduction of FDG uptake in any part of the baboon brain when subtracting the OFF from the ON states.

Electrophysiological Changes

The current model of basal ganglia dysfunction in PD suggests that abnormal overactivity of output nuclei such as the STN and the GPi accounts for motor symptoms in this disorder (DeLong, 1990; Wichmann and DeLong, 1999). To determine if MCS could normalize neuronal electrical activities in basal ganglia output regions, normal and MPTP-treated baboons with severe ^{18}F-DOPA depletion underwent simultaneous unitary recordings in both GPi and STN, just before being sacrificed for postmortem histological analysis. In agreement with previous reports (DeLong, 1990), we found a significant increase in the mean firing rate of GPi and STN neurons in MPTP-treated baboons in OFF condition compared to controls (GPi, 65.7 $\pm$ 3.3 Hz [n = 16] versus 35.8 $\pm$ 1.3 Hz [n = 48]; and STN, 27.6 $\pm$ 1.7 Hz [n = 32] versus 15.7 $\pm$ 0.7 Hz [n = 62]; Mann-Whitney test [MW], $p < 0.0001$) (Figure 3A and Figure 5A).

After removal of the stimulation artifact by template subtraction methods (Hashimoto et al., 2002), MCS significantly reduced abnormal high firing rates in MPTP GPi neurons (Figure 4A) during 1 min MCS (65.7 $\pm$ 3.3 Hz [n = 16] [MPTP PRE] versus 32.8 $\pm$ 4.2 Hz [n = 9] [PER]; WSR, $p < 0.01$) (Figures 3A and 3C and Figure 4B), restoring normal firing rate values in this structure (32.8 $\pm$ 4.2 Hz [n = 9] [PER] versus 35.8 $\pm$ 1.3 Hz [n = 48] [control]; MW, $p > 0.3$). This effect persisted up to 1 min after the cessation of MCS (65.7 $\pm$ 3.3 Hz [n = 16] [MPTP PRE] versus 42.1 $\pm$ 3.4 Hz [n = 14] [POST1]; WSR, $p < 0.01$) (Figure 3A). MCS effects on GPi firing rate were reversible, as abnormal firing rate reappeared in the same neurons within 5 min post-MCS (Figure 3A and Figure 4B). Whereas in one severely disabled MPTP baboon, electrophysiological recordings in the GPi contralateral to the cortical electrode stimulation showed that the mean firing rates in this structure were equally elevated as compared to the ipsilateral GPi neurons following MPTP intoxication (50.1 $\pm$ 7.2 Hz [n = 6] [MPTP PRE] versus 65.7 $\pm$ 3.3 Hz [n = 16] [MPTP PRE] respectively; MW, $p > 0.05$); this hyperactivity was also normalized during the 1 min MCS stimulation (50.1 $\pm$ 7.2 Hz [MPTP PRE] versus 37.4 $\pm$ 5.1 Hz [PER] [n = 6]; WSR, $p < 0.05$) but not after switching OFF the stimulator (50.1 $\pm$ 7.2 Hz [MPTP PRE] versus 45.3 $\pm$ 4 Hz [POST1] [n = 6]; WSR, $p > 0.2$) (Figure 3C).

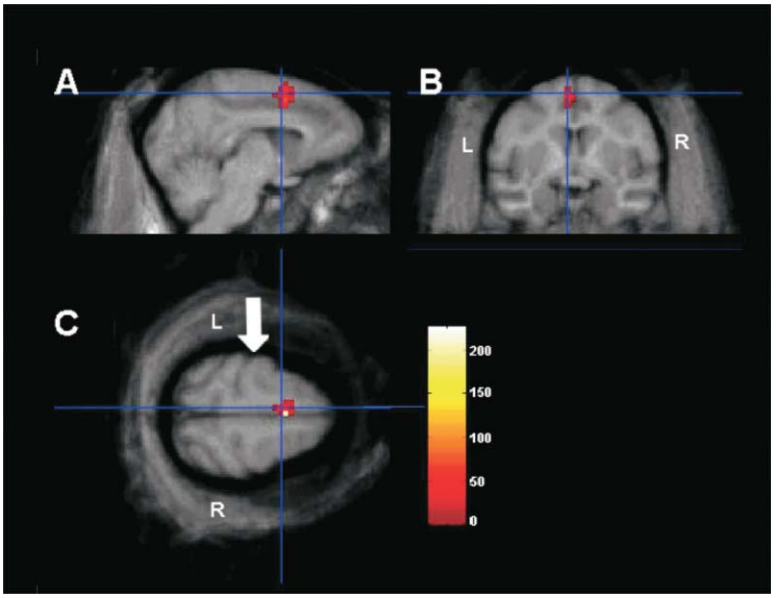

Figure 2. MCS Increases Brain Metabolism ^{18}F-FDG Uptake in the Mesial Premotor Cortex of Parkinsonian Baboons

Sagittal (A), coronal (B), and axial (C) views of merged PET statistical maps and baboon's MRI volumes showing a significant increase of brain metabolism (^{18}FDG-PET) in the ipsilateral SMA and dorsal motor cingulum during MCS (red colors indicate all pixels displaying a significant increase [$p < 0.05$] between ON and OFF MCS condition). Blue lines points to the SMA ipsilateral to the MCS's electrode; white arrow, stimulated primary motor cortex.

In MPTP STN neurons, after removal of the stimulation artifact, MCS also significantly normalized STN firing rates during 1 min MCS, an effect that persisted up to 1 min following termination of the MCS (27.6 ± 1.7 Hz [n = 32] [MPTP PRE] versus 17 ± 2.3 Hz [n = 23] [PER]; WSR, $p < 0.01$) (Figure 4C and Figure 5A). MCS's effects in the STN appeared rather heterogeneous depending on the baseline firing rate measured in the prestimulation period. Indeed, only STN neurons that were considered as "hyperactive" (exhibiting a firing rate 2 standard deviations [23 Hz] above mean firing rate measured in control animals) significantly decreased their mean discharge rate before and 1 min after MCS, while STN neurons displaying a firing rate within the normal range remained unaffected both during MCS and at any time after MCS (Figures 5C and 5D). Also, MCS's effects on STN firing rate were reversible, as abnormal firing rate reappeared in the same neurons within 3–5 min post-MCS (Figure 4C and Figure 5A). In marked contrast with these observations in parkinsonian baboons, MCS had no effect on the discharge rate of either GPi (35.8 ± 1.3 Hz [n = 48] [PRE] versus 34.7 ± 1.7 [n = 22] [PER]; WSR, $p > 0.05$) or STN neurons (15.7 ± 0.7 Hz [n = 62] [PRE] versus 15.1 ± 1.4 [n = 19] [PER]; WSR, $p > 0.5$), in nonlesioned control animals (Figure 3B and Figure 5B).

Pattern analysis of neuronal discharges was performed only after the completion of MCS trains to avoid any misinterpretation with the removal of stimulation artifact (see Experimental Procedures). Thus, pattern analysis revealed that although the proportion of oscillating cells in the STN was similar in both MPTP primates (18/21; 86%) and control animals (45/49; 92%; χ^2 test, $p > 0.4$), oscillating GPi neurons were more abundant in MPTP primates (13/16) compared to controls (17/38) (45% versus 81%; χ^2 test, $p < 0.05$). Additionally, GPi and STN neurons were more prone to discharge synchronously in MPTP primates, since the number of synchronized pairs (13/18) was higher compared to control animals (4/15) (χ^2 test, $p < 0.01$).

One minute MCS significantly decreased the number of oscillating neurons in both GPi neurons (81% [13/16] [PRE] versus 46% [6/13] [POST]; χ^2 test, $p < 0.05$) and STN neurons (86% [18/21] [PRE] versus 55% [11/20] [POST]; χ^2 test, $p < 0.05$), as compared to results obtained in the OFF condition (Figure 6B). Finally, MCS significantly reduced the number of synchronized pairs of neurons between the two structures (72% [OFF] versus 39% [ON]; χ^2 test, $p < 0.01$). Again, these effects of MCS were specific to the MPTP-treated monkeys, as no significant effects of MCS were observed either on the number of oscillating neurons per structures (GPi, 45% [OFF] versus 57% [ON], χ^2 test, $p > 0.2$; STN, 92% [OFF] versus 85% [ON], χ^2 test, $p > 0.2$) or the number of synchronized pairs of neurons between structures (27% [OFF] versus 40% [ON]; χ^2 test, $p > 0.5$).

Postmortem histological analysis confirmed that all MPTP-treated animals displayed a prominent loss of tyrosine hydroxylase immunoreactivity (TH-ir) in both striatum and substantia nigra pars compacta (Figure 1G). Searching for possible deleterious effects of chronic MCS, we performed acetylcholine-esterase (AchE) histochemistry and Nissl staining. Except for the narrow area surrounding the recording needle tracks in the STN or the GPi, no cell loss or inflammatory response was observed in any area of the brain, including the stimulated region on the left primary motor cortex.

Discussion

The most salient finding in the above series of experiments is the demonstration that electrical modulation of the motor cortex, using low-voltage/high-frequency trains of pulses at an intensity below threshold for muscle twitching, induces significant reversal of parkinsonism in MPTP-treated baboons. This result was obtained in the absence of any side effects, using an epidural electrode that can be introduced without a deep brain stereotaxic approach and checked, for its precise placement, using conventional neurophysiological techniques. Accordingly, motor cortex stimulation appears to be a

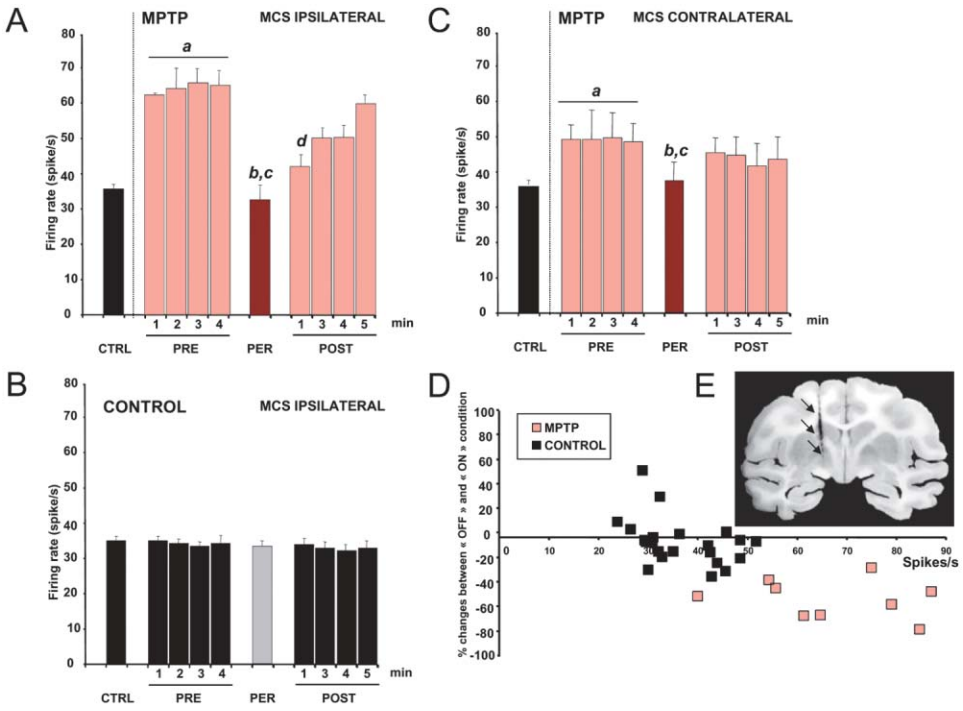

Figure 3. MCS's Effects on Control and MPTP GPi Neurons

(A) Mean firing rate of GPi neurons ipsilateral to MCS recorded in controls (black bars) and in MPTP animals before MCS (PRE, orange bars), during 1 min MCS (PER, brown bar), and after MCS (POST, orange bars). As compared to control GPi neurons, an increased firing frequency was observed in GPi neurons of MPTP animals. One minute MCS (PER) restored normal firing rate in MPTP GPi neurons, which progressively returned to PRE stimulation levels by 3 min post-MCS. (MW, $p < 0.05$, [a]PRE versus CTRL; MW, n.s., [b]PER versus CTRL; WSR, $p < 0.05$, [c]PER versus PRE; and WSR, $p < 0.05$, [d]POST 1′ versus PRE). Each bar indicates a 20 s period of analysis.

(B) Mean firing rate of GPi neurons ipsilateral to MCS recorded in control animals (black bars). Note that no change in mean discharge frequency was observed either during (PER, gray bar) or at any time after MCS (POST), compared to the OFF condition (PRE).

(C) Mean firing rate of GPi neurons contralateral to MCS recorded in one MPTP animal before MCS (PRE, orange bars), during MCS (PER, brown bar), and after MCS (POST, orange bars). One minute MCS significantly reduced the firing rate of contralateral GPi neurons only during MCS (PER). Abnormally increased firing rate immediately returned to PRE MCS levels after switching OFF the stimulator. (MW, $p < 0.05$, [a]PRE versus CTRL; MW, n.s., [b]PER versus CTRL; WSR, $p < 0.05$, [c]PER versus PRE).

(D) Scatter plot diagram representing the percent change in mean firing rate of 9 MPTP and 22 control GPi neurons between OFF and ON conditions, plotted against their respective basal mean firing frequency measured in OFF condition. Note that 1 min MCS reduced firing rates in all MPTP GPi neurons (orange dots), whereas it had no major effect on control GPi neurons (black dots).

(E) Images obtained while cutting the brain on the sliding microtome. Up to 2300 images of the frozen brain slices (40 μm thick) were digitized and sum up to yield a three-dimensional (3D) volume of each baboon's brain using Baladin software (from Epidaure, Inria Sophia Antipolis, France), a software based on a robust block-matching strategy (Ourselin et al., 2001). Final images were obtained by restoring the 3D volume to display the entire course of GPi track (arrows).

potential alternative to deep brain stimulation in the STN or GPi, with major advantages in terms of simplicity and safety of the procedure.

Whether MCS can be as efficient as STN or GPi electrical stimulation to alleviate motor symptoms in PD patients is a question that will require specifically designed comparative clinical trials. Nevertheless, the results obtained here in baboons strongly suggest that this may be the case. First, unilateral MCS can significantly improve akinesia and bradykinesia in MPTP-treated monkeys with severe bilateral dopamine depletion. Although experimental conditions were different, a similar behavioral benefit was previously reported with unilateral high-frequency STN stimulation in an acute unilateral primate model of PD (Benazzouz et al., 1993). Second, the motor benefits induced by unilateral MCS were associated with normalization of mean firing rates and aberrant neuronal activities typically observed within and between STN and GPi neurons in MPTP primate models and PD patients (Heimer et al., 2002; Levy et al., 2002). Moreover, the symmetrical motor recovery observed following unilateral MCS in the present study was also associated with normalization of abnormal firing rates in both ipsilateral and contralateral GPi neurons. According to current theories of basal ganglia dysfunction, it has been proposed that those aberrant neuronal activities downstream of the striatum may play a critical role in the emergence of motor symptoms (Wichmann and DeLong, 1999). By normalizing those activities, MCS may indirectly reproduce the inhibitory effects also obtained in rat model of PD and parkinsonian patients through direct deep brain stimulation of STN (Tai et al., 2003; Welter et al., 2004).

It is noteworthy that, whereas the effects of MCS on the neuronal firing rates in the STN or the GPi were almost immediate (observed within the first minute of stimulation), the clinical benefit of MCS on symptoms such as akinesia or bradykinesia necessitated a longer

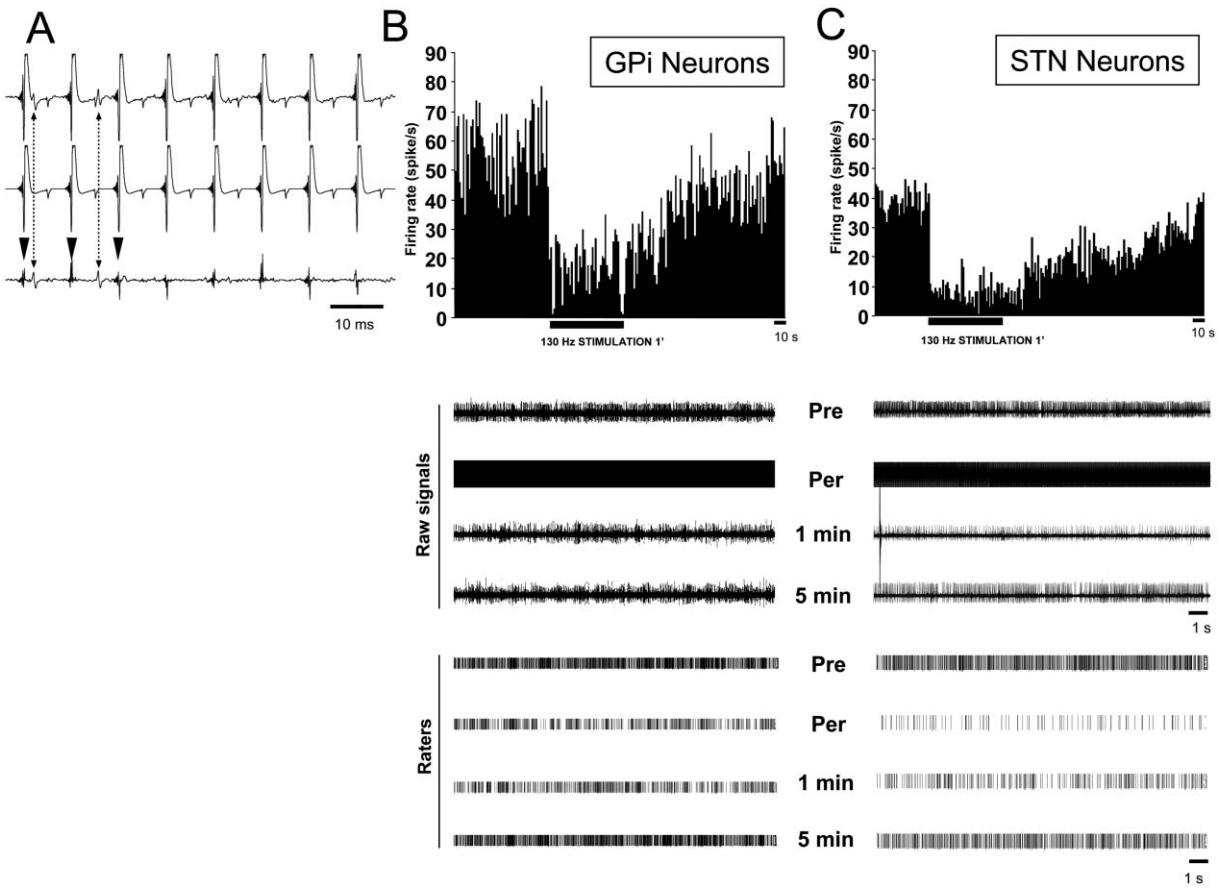

Figure 4. Artifact Removal Procedure and Resulting Representations of GPi and STN Neurons' Raw Traces

(A) (Upper trace) Representative example of a STN neuron recorded during MCS before artifact subtraction. (Middle trace) Artifact template constructed with the average artifact waveform synchronized with the raw trace. (Lower trace) Signal remaining following artifact subtraction, in which spikes are easily discernable (dashed arrows). Arrowheads indicate the residual artifacts of MCS that can be easily discriminated from the actual spikes (dashed arrows).

(B) (Upper panel) Instantaneous firing rate recorded in GPi neuron before, during, and 3 min after MCS at 130 Hz. (Lower panels) Raw signals before (PRE), during (PER), and 1 and 5 min after MCS, with their corresponding rasters.

(C) (Upper panel) Instantaneous firing rate recorded in STN neuron before (PRE), during (PER), and 1 and 5 min after MCS at 130 Hz. (Lower panels) Raw signals before (PRE), during (PER), and 3 min after MCS, with their corresponding rasters.

stimulation time to become detectable. The latency of the clinical effects of high-frequency deep brain stimulation of the STN is also known to vary from one type of parkinsonian motor symptoms to another with short latency benefit (less than 1 min) observed for rigidity and tremor and longer time delay (a few minutes, up to a few days) observed for other symptoms such as bradykinesia and akinesia (Krack et al., 2002). In contrast to this delay, the effects of high-frequency deep brain stimulation on the neuronal firing rates recorded directly in the STN are almost immediate after the stimulator is turned ON (Welter et al., 2004; Dostrovsky et al., 2000). As discussed by others, these uneven behavioral delays observed with both MCS and deep brain stimulation may be due to different mechanisms such as secondary messengers or long-term potentiation of stimulation (Temperli et al., 2003; Krack et al., 2002).

Finally, PET imaging data indicate that MCS also affects cortical regions, particularly those implicated in movement initiation. Indeed, functional hypoactivity of the mesial premotor cortex is a hallmark of akinesia in PD patients and primate model of PD (Bezard et al., 2001; Escola et al., 2003; Playford et al., 1992). These cortical metabolic abnormalities can be reversed by antiparkinsonian therapies such as dopaminergic treatment (Jenkins et al., 1992), pallidotomy (Grafton et al., 1995), or high-frequency stimulation of the STN (Limousin et al., 1997) or of the GPi (Fukuda et al., 2001). The similarity of the present data with MCS in MPTP-treated baboons further suggests that this strategy may induce a similar therapeutic benefit in PD patients. These experimental findings also support the need to assess cortical stimulation in other neurological and neuropsychiatric disorders in which cortico-basal loop dysfunction is suspected (Llinas et al., 1999).

Experimental Procedures

Animals

Studies were conducted in accordance with the European convention for animal care (86-406) and the guide for the care and use of laboratory animals adopted by the National Institutes of Health. Seven adult baboons (*Papio papio*), 15 kg body weight, were in-

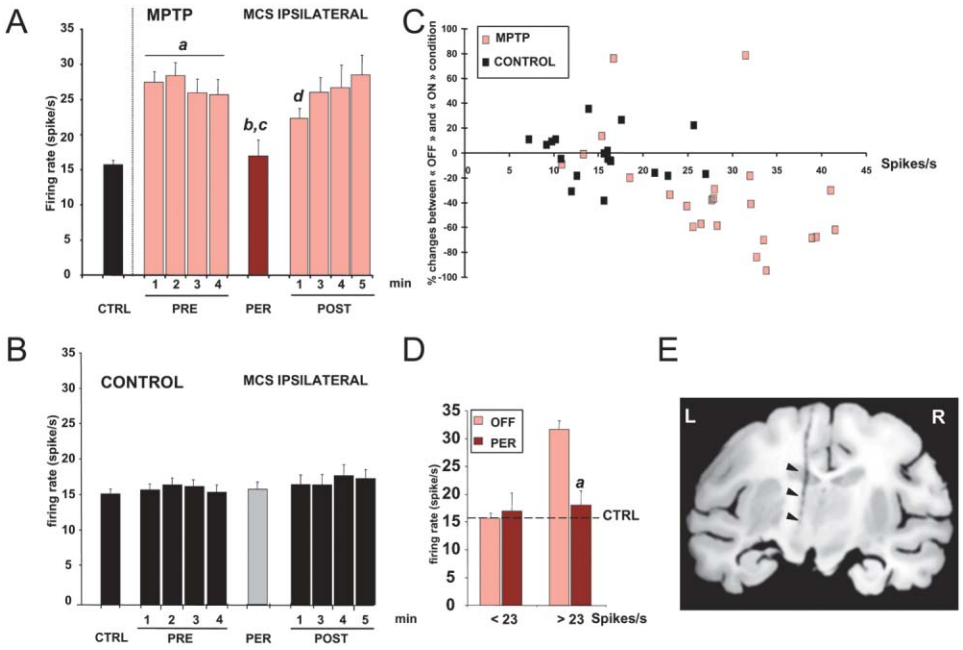

Figure 5. MCS's Effects on Control and MPTP STN Neurons

(A) Mean firing rate of STN neurons ipsilateral to MCS recorded in controls (black bars) and in MPTP animals before MCS (PRE, orange bars), during 1 min MCS (PER, brown bars), and after MCS (POST, orange bars). As compared to control STN neurons, an increased firing frequency was observed in STN neurons of MPTP animals. One minute MCS (PER) restored normal firing rate in MPTP STN neurons, which progressively returned to the PRE stimulation levels by 3 min post-MCS. (MW, $p < 0.05$, [a]PRE versus CTRL; MW, n.s., [b]PER versus CTRL; WSR, $p < 0.05$, [c]PER versus PRE; and WSR, $p < 0.05$, [d]POST versus PRE).

(B) Mean firing rate of STN neurons ipsilateral to MCS recorded in control animals (black bars). Note that no change in mean discharge frequency was observed either during (PER, gray bar) or after MCS (POST) compared to the OFF condition (PRE).

(C) Scatter plot diagram representing the percent change in mean firing rate of 23 MPTP and 19 control STN neurons between OFF and ON conditions, plotted against their respective basal mean firing frequency in OFF conditions. Note that MCS reduced firing rate in the majority of MPTP STN neurons (orange squares), whereas it had no major effect on control STN neurons (black squares) and "normoactive" STN neurons (brown squares).

(D) Whereas "normoactive" STN neurons (i.e., with firing rate <23 Hz) remained unaffected by MCS, firing frequency of "hyperactive" STN neurons (i.e., with firing rate >23 Hz) significantly diminished during MCS (WSR, [a]$p < 0.05$). Dashed line indicates the average level of STN firing frequency observed in nonlesioned control animals.

(E) STN track (arrows) obtained after 3D reconstruction of the histological volume.

cluded in this study. All animals were housed individually in standard primate cages with free access to water and food.

Experimental Design

A four-contact Resume electrode (Medtronic model 3587A; Minneapolis, MN) was placed flat over the dura mater along the left precentral gyrus (M1) in seven adult *Papio papio* baboons (two controls, five MPTP-treated). The electrode was then connected to a subcutaneous pulse generator (Medtronic model 7424; Minneapolis, MN). The precise location of each contact over the motor cortex was verified using motor-evoked potentials induced by the neurostimulator generating pulses above motor threshold. The flow chart of the full experiment involved, for three MPTP-treated animals, a complete study involving daily clinical assessment, plus a series of behavioral and functional imaging analyses with PET, before any MPTP administration and during a 52 week long systemic MPTP intoxication paradigm. Two additional MPTP-treated animals were included in the imaging and electrophysiological studies. Two animals were kept unlesioned and served as controls for electrophysiology and histology. Electrophysiological recordings in the STN and GPi were performed in the final stage of the experiments, before the animals were sacrificed and their brains were analyzed using histological techniques.

Surgery

Following a burr hole drilled in the skull overlying the area of interest, each baboon received an unilateral epidural implantation of a Resume electrode along the left primary motor cortex, under MRI guidance using a 1.5 magnet (General Electric Medical Systems, Waukesha, WI). The electrode was connected to a pulse generator that could be programmed externally with respect to electrode contact (four sites), polarity (monopolar or bipolar), frequency (up to 185 Hz), voltage (up to 10.5 V), and pulse width (up to 450 μs). Motor-evoked potentials were recorded using needle electrodes placed subcutaneously in the right hemi-face, shoulder, wrist, and fingers. An average of 2 V cathodal monopolar stimulations (160 μs; 2 Hz) induced contralateral muscle twitches. Motor threshold was established as the minimal intensity eliciting at least five muscle twitches in response to ten electrical pulses. The intensity of the cortical stimulation was then set at 80% of this motor threshold.

MPTP Neurotoxic Treatment

Four of the six baboons received an initial daily dose of 0.2 mg/kg MPTP (Sigma Aldrich, St. Louis, MO) for 9 days. Because partial behavioral recovery occurring within 1 month following the cessation of MPTP treatment can frequently be observed in acutely intoxicated animals, baboons were then submitted to a long-term neurotoxic treatment consisting in weekly intramuscular injections of MPTP with a starting dose at 0.5 mg/kg and increments of 0.1 mg/kg every 2 weeks until 1 mg/kg was reached (Poyot et al., 2001). Weekly injections of MPTP (1 mg/kg) were then administered over the entire experimental period to maintain a severe steady parkinsonism. During the entire time course of the MPTP intoxication, animals were imaged monthly with ^{18}F-DOPA PET scans. One additional baboon

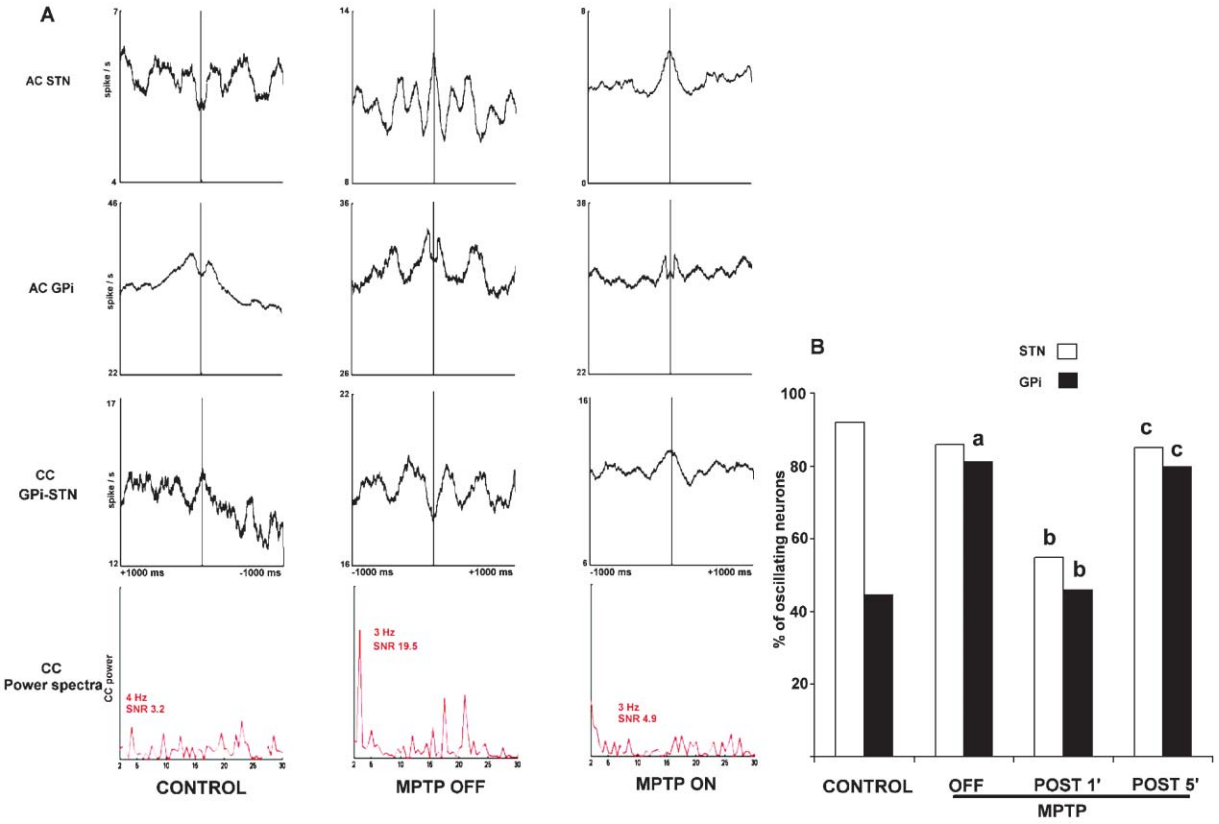

Figure 6. MCS Reduces the Number of Oscillating Neurons and Synchronized Pairs in the MPTP STN and GPi

(A) (From top to bottom) Representative auto-correlogram (AC) in STN and GPi neurons, cross-correlogram (CC) of STN-GPi pairs of neurons simultaneously recorded, and power spectra of cross-correlogram (CC-power) obtained in one control animal (left), one MPTP animal in OFF condition (center), and the same MPTP animal 1 min post-MCS (right). AC in the STN and GPi returned to a nonoscillatory state 1 min after MCS compared to AC performed in the same MPTP animal under OFF condition. Power spectra of CC showed a significant peak at 3 Hz frequency in MPTP OFF condition that disappeared 1 min after MCS.

(B) Histogram showing the percentage of oscillating neurons in the MPTP STN and GPi. MCS significantly reduced the number of oscillating neurons observed in MPTP OFF condition, in both STN and GPi at 1 min post-MCS. (χ^2 test, $^a p < 0.05$, control versus MPTP OFF; $^b p < 0.05$, MPTP OFF versus ON 1 min post-MCS; $^c p < 0.05$, ON 1 min post-MCS versus ON 5 min post-MCS).

received a systemic daily dose of 0.2 mg/kg MPTP until the animal reached a severe parkinsonian state.

Behavioral Assessment

Animals were videotaped in special video cage for 30 min every week for the first 10 weeks post-MPTP, then every 4 weeks when ^{18}F-DOPA PET scan was performed. A telemetric programmer (Medtronic model 7432; Minneapolis, MN) allowed switching the pulse generator ON or OFF without anesthesia. Tapes were analyzed offline by an examiner blinded to the experiment condition for qualitative evaluation using a clinical rating score adapted from previous scales (Baron et al., 2002; Papa and Chase, 1996). Briefly, severity of general akinesia (0–5), right upper limb agility (0–5), general bradykinesia (0–4), climbing abilities (0–4), tremor (0–2), gait (0–2), and posture (0–2) were rated (maximal score, 24). Number of walking initiation and climbing behavior were also quantified during the 30 min time period. Walking initiation was counted when animal initiated a displacement of at least three steps after at least 4 s of immobilization. A climbing behavior was counted when animal climbed up or down or moved along the wall after at least 4 s of immobilization.

Video-based motion tracking and analyzing system (Ethovision, Noldus, Wageningen, the Netherlands) allowed objective measurement of TDM and MV during 30 min period. TDM measured akinesia, and MV reflected bradykinesia (Hantraye et al., 1996). The ON/OFF TDM ratio was measured for each video sequence to quantify the degree of motor recovery, a ratio of one indicating no behavioral effect.

Imaging Studies

PET scans were performed in 3D mode using the ECAT EXACT HR+ high-resolution tomograph (CTI-Siemens, Knoxville, TN), which acquires 63 contiguous planes simultaneously. A transmission scan was performed for attenuation correction. Animals were anesthetized with a mixture of ketamine/xylazine (15 mg/1.5 mg/kg) followed by isoflurane 2% in a NO_2/O_2 mixture (NO_2/O_2 = 3/2) for FDG. Baboons were positioned in a stereotactic frame aligned with crossed laser beams permanently attached on the tomograph to ensure an exact repositioning of the head in different PET sessions.

Striatal dopaminergic function was assessed using ^{18}F-DOPA as described elsewhere (Poyot et al., 2001). ^{18}F-DOPA (3.5 ± 0.2 mCi) was administered over 30 s, and 90 min three-dimensional dynamic emission scan started. Regions of interest (ROI) were placed on the putamen and cerebellum. Cerebellar activity was used as a nonspecific input function to generate maps of the uptake rate constant (Ki) using the modified graphical method (Patlak and Blasberg, 1985). Striatal ROIs were transferred to the functional maps, and the Ki values were evaluated as the ROI means for each structure.

MCS impact on cerebral metabolism was measured with PET scans using FDG as a tracer. Two FDG PET scans on 2 separate days were performed OFF and ON stimulation with the same parameters employed for the behavioral study. A 60 min emission scan con-

sisting of 28 frames was obtained following intravenous injection of 4.5 ± 0.2 mCi of FDG. Images of each subject were summed, realigned to the first volume, and normalized to blood flow PET template, and all voxels within the brain were examined using statistical parametric mapping (SPM99; Wellcome Department of Cognitive Neurology, London, UK). Significant changes in regional cerebral FDG uptake were identified by comparing images obtained in the two conditions (OFF and ON) on a voxel-by-voxel basis with *t* statistics. Comparisons were specified by the use of two categorical contrasts ("OFF-ON" and "ON-OFF"). These analyses generated SPM {*t*} maps and subsequent SPM {*Z*} maps, where clusters of voxels that had a peak *Z* score of >6.31 (threshold $p < 0.05$, uncorrected for multiple comparison) were considered to show significant activation and appear colored on SPM maps.

Electrophysiological Recordings

Under constantly monitored ketamine/xylazine anesthesia (15 mg/1.5 mg/kg), single-unit activities were recorded only during time period with stable heart rate, respiratory frequency, and CO2 expiratory flow. Two glass-coated tungsten microelectrodes were stereotactically implanted under MRI guidance into the GPi and STN. Recording locations were verified by histological reconstruction of the electrode tracks. Signal was amplified and band-pass filtered (300–5000 Hz) using Leadpoint (Medtronic, Minneapolis, MN). Single-cell action potentials were first threshold extracted, and only well-isolated units with a constant firing rate for at least 3 min were selected for further analysis. Twenty second spike trains were recorded before, during, and 1, 3, 4, and 5 min after 1 min 130 Hz MCS and stored for offline analysis. In the present study, we choose to analyze 1 min time period during stimulation because it represented a good compromise between the time of stimulation necessary to characterize the effect of MCS on individual neuronal firing rates and the necessary statistical requirement of recording a great number of neurons within each brain region of interest during a single experiment. Selecting 1 min MCS implied that we study a single neuron for at least 9–10 min (total recording time of a single neuron), which corresponds to 3–4 min recording under baseline condition, 1 min recording during MCS, and 5 min recording poststimulation. Because of the relative persistency of the MCS effects, the latter time period of 5 min poststimulation was absolutely necessary to observe the total disappearance of the MCS's effects on neuronal firing rate before starting another neuronal recording.

Electrophysiological Analysis

Neuronal activity was extracted using a template-matching algorithm (Dataview4.5; W.J. Heitler, University of St. Andrews, Scotland), and mean firing rates were calculated. Auto- and cross-correlograms were constructed after subtracting the baseline firing rate with a ±1000 ms offset (1 ms bin size; Matlab subroutines; The MatWorks, Natick, MA). Periodic oscillations were detected using the power spectra of the correlograms (Raz et al., 2000). Units were considered oscillatory if a significant peak (with a signal-to-noise ratio >5) was found in the power spectrum between 3 and 19 Hz (Raz et al., 2000).

Stimulation Artifact Subtraction

The stimulus artifact contained a complex multiphasic potential that was 1.8–2.3 ms in duration and was relatively large compared to the amplitude of neuronal spikes. To downscale the stimulation artifact, we used an offline subtraction method derived from Hashimoto et al. (2002). Briefly, once a well-isolated unit was identified and after a 3 min baseline period had been registered, neuronal activity during a 1 min period of 130 Hz MCS was recorded and stored for analysis ("PER stimulation period"). Using an offline template recognition algorithm (Dataview 4.5; W.J. Heitler, University of St. Andrews, Scotland) stimulation artifacts were identified (near 7800 artifacts per trace) on the raw trace. Then, a template established from the average of all the 7800 artifact waveforms was created. Next, a trace was constructed with a train of this average artifact waveform, synchronized to each artifact of the raw trace. Between artifact waveforms, the trace has a value of zero (Figure 4A). Finally, the artifact trace was subtracted from the raw trace to recover the neuronal signal recorded during the stimulation period. This procedure did not completely eliminate artifacts but considerably reduced their duration and amplitude and lengthened the period during which neuronal activity could be discriminated. Because small residual artifacts remained detectable, the entire subtracted trace was visually and carefully inspected for spike detection. In addition, because spike detection was effective only in the period free of residual artifact, and because this "blind period" occurred regularly and not randomly, we build auto- and cross-correlograms only after the stimulation period.

Histology

Animals were transcardially perfused with 4% paraformaldehyde, and their brains were processed for immunohistochemistry as described elsewhere (Poyot et al., 2001). One section out of 18 was processed for acetylcholine-esterase histochemistry, Nissl staining, and tyrosine hydroxylase immunodetection (Institute Jacques Boy, France; 1:3000) using the avidin-biotin method as previously described (Poyot et al., 2001).

Acknowledgments

This research was partly supported by Medtronic Inc. X.D. was supported by fellowships from Assistance Publique-Hôpitaux de Paris; Association des Journées de Neurologie de Langue Française; and Association pour la Recherche sur la stimulation cérébrale. We deeply thank Pr. Yves Agid and Dr. Liza Leventhal for reviewing the manuscript. We thank J.C. Sol, M.C. Gregoire, J.B. Gallezot, W. Saada, R. Maroy, and F. Gerraz for technical assistance; and C. Jouy and F. Sergent for excellent animal care.

Received: October 10, 2003
Revised: July 21, 2004
Accepted: November 4, 2004
Published: December 1, 2004

References

Baron, M.S., Wichmann, T., Ma, D., and DeLong, M.R. (2002). Effects of transient focal inactivation of the basal ganglia in parkinsonian primates. J. Neurosci. *22*, 592–599.

Bejjani, B.P., Damier, P., Arnulf, I., Thivard, L., Bonnet, A.M., Dormont, D., Cornu, P., Pidoux, B., Samson, Y., and Agid, Y. (1999). Transient acute depression induced by high-frequency deep-brain stimulation. N. Engl. J. Med. *340*, 1476–1480.

Benazzouz, A., Gross, C., Feger, J., Boraud, T., and Bioulac, B. (1993). Reversal of rigidity and improvement in motor performance by subthalamic high-frequency stimulation in MPTP-treated monkeys. Eur. J. Neurosci. *5*, 382–389.

Bevan, M.D., Magill, P.J., Terman, D., Bolam, J.P., and Wilson, C.J. (2002). Move to the rhythm: oscillations in the subthalamic nucleus-external globus pallidus network. Trends Neurosci. *25*, 525–531.

Bezard, E., Crossman, A.R., Gross, C.E., and Brotchie, J.M. (2001). Structures outside the basal ganglia may compensate for dopamine loss in the presymptomatic stages of Parkinson's disease. FASEB J. *15*, 1092–1094.

DeLong, M.R. (1990). Primate models of movement disorders of basal ganglia origin. Trends Neurosci. *13*, 281–285.

Dostrovsky, J.O., Levy, R., Wu, J.P., Hutchison, W.D., Tasker, R.R., and Lozano, A.M. (2000). Microstimulation-induced inhibition of neuronal firing in human globus pallidus. J. Neurophysiol. *84*, 570–574.

Escola, L., Michelet, T., Macia, F., Guehl, D., Bioulac, B., and Burbaud, P. (2003). Disruption of information processing in the supplementary motor area of the MPTP-treated monkey: a clue to the pathophysiology of akinesia? Brain *126*, 95–114.

Fukuda, M., Mentis, M., Ghilardi, M.F., Dhawan, V., Antonini, A., Hammerstad, J., Lozano, A.M., Lang, A., Lyons, K., Koller, W., et al. (2001). Functional correlates of pallidal stimulation for Parkinson's disease. Ann. Neurol. *49*, 155–164.

Goldberg, J.A., Boraud, T., Maraton, S., Haber, S.N., Vaadia, E., and Bergman, H. (2002). Enhanced synchrony among primary motor

cortex neurons in the 1-methyl-4-phenyl-1,2,3,6-tetrahydropyridine primate model of Parkinson's disease. J. Neurosci. *22*, 4639–4653.

Grafton, S.T., Waters, C., Sutton, J., Lew, M.F., and Couldwell, W. (1995). Pallidotomy increases activity of motor association cortex in Parkinson's disease: a positron emission tomographic study. Ann. Neurol. *37*, 776–783.

Hantraye, P., Brouillet, E., Ferrante, R., Palfi, S., Dolan, R., Matthews, R.T., and Beal, M.F. (1996). Inhibition of neuronal nitric oxide synthase prevents MPTP-induced parkinsonism in baboons. Nat. Med. *2*, 1017–1021.

Hashimoto, T., Elder, C.M., and Vitek, J.L. (2002). A template subtraction method for stimulus artifact removal in high-frequency deep brain stimulation. J. Neurosci. Methods *113*, 181–186.

Heimer, G., Bar-Gad, I., Goldberg, J.A., and Bergman, H. (2002). Dopamine replacement therapy reverses abnormal synchronization of pallidal neurons in the 1-methyl-4-phenyl-1,2,3,6-tetrahydropyridine primate model of parkinsonism. J. Neurosci. *22*, 7850–7855.

Houeto, J.L., Mesnage, V., Mallet, L., Pillon, B., Gargiulo, M., du Moncel, S.T., Bonnet, A.M., Pidoux, B., Dormont, D., Cornu, P., and Agid, Y. (2002). Behavioural disorders, Parkinson's disease and subthalamic stimulation. J. Neurol. Neurosurg. Psychiatry *72*, 701–707.

Jenkins, I.H., Fernandez, W., Playford, E.D., Lees, A.J., Frackowiak, R.S., Passingham, R.E., and Brooks, D.J. (1992). Impaired activation of the supplementary motor area in Parkinson's disease is reversed when akinesia is treated with apomorphine. Ann. Neurol. *32*, 749–757.

Krack, P., Pollak, P., Limousin, P., Hoffmann, D., Xie, J., Benazzouz, A., and Benabid, A.L. (1998). Subthalamic nucleus or internal pallidal stimulation in young onset Parkinson's disease. Brain *121*, 451–457.

Krack, P., Fraix, V., Mendes, A., Benabid, A.L., and Pollak, P. (2002). Postoperative management of subthalamic nucleus stimulation for Parkinson's disease. Mov. Disord. Suppl. *17*, S188–S197.

Levy, R., Ashby, P., Hutchison, W.D., Lang, A.E., Lozano, A.M., and Dostrovsky, J.O. (2002). Dependence of subthalamic nucleus oscillations on movement and dopamine in Parkinson's disease. Brain *125*, 1196–1209.

Limousin, P., Greene, J., Pollak, P., Rothwell, J., Benabid, A.L., and Frackowiak, R. (1997). Changes in cerebral activity pattern due to subthalamic nucleus or internal pallidum stimulation in Parkinson's disease. Ann. Neurol. *42*, 283–291.

Limousin, P., Krack, P., Pollak, P., Benazzouz, A., Ardouin, C., Hoffmann, D., and Benabid, A.L. (1998). Electrical stimulation of the subthalamic nucleus in advanced Parkinson's disease. N. Engl. J. Med. *339*, 1105–1111.

Llinas, R.R., Ribary, U., Jeanmonod, D., Kronberg, E., and Mitra, P.P. (1999). Thalamocortical dysrhythmia: A neurological and neuropsychiatric syndrome characterized by magnetoencephalography. Proc. Natl. Acad. Sci. USA *96*, 15222–15227.

Magill, P.J., Bolam, J.P., and Bevan, M.D. (2001). Dopamine regulates the impact of the cerebral cortex on the subthalamic nucleus-globus pallidus network. Neuroscience *106*, 313–330.

Ourselin, S., Roche, A., Subsol, G., Pennec, X., and Ayache, N. (2001). Reconstructing a 3D structure from serial histological sections. Image Vis. Comput. *19*, 25–31.

Papa, S.M., and Chase, T.N. (1996). Levodopa-induced dyskinesias improved by a glutamate antagonist in Parkinsonian monkeys. Ann. Neurol. *39*, 574–578.

Patlak, C.S., and Blasberg, R.G. (1985). Graphical evaluation of blood-to-brain transfer constants from multiple-time uptake data. Generalizations. J. Cereb. Blood Flow Metab. *5*, 584–590.

Playford, E.D., Jenkins, I.H., Passingham, R.E., Nutt, J., Frackowiak, R.S., and Brooks, D.J. (1992). Impaired mesial frontal and putamen activation in Parkinson's disease: a positron emission tomography study. Ann. Neurol. *32*, 151–161.

Poyot, T., Conde, F., Gregoire, M.C., Frouin, V., Coulon, C., Fuseau, C., Hinnen, F., Dolle, F., Hantraye, P., and Bottlaender, M. (2001). Anatomic and biochemical correlates of the dopamine transporter ligand 11C-PE2I in normal and parkinsonian primates: comparison with 6-[18F]fluoro-L-dopa. J. Cereb. Blood Flow Metab. *21*, 782–792.

Raz, A., Vaadia, E., and Bergman, H. (2000). Firing patterns and correlations of spontaneous discharge of pallidal neurons in the normal and the tremulous 1-methyl-4-phenyl-1,2,3,6-tetrahydropyridine vervet model of parkinsonism. J. Neurosci. *20*, 8559–8571.

Ribeiro, M.J., Vidailhet, M., Loc'h, C., Dupel, C., Nguyen, J.P., Ponchant, M., Dolle, F., Peschanski, M., Hantraye, P., Cesaro, P., et al. (2002). Dopaminergic function and dopamine transporter binding assessed with positron emission tomography in Parkinson disease. Arch. Neurol. *59*, 580–586.

Tai, C.H., Boraud, T., Bezard, E., Bioulac, B., Gross, C., and Benazzouz, A. (2003). Electrophysiological and metabolic evidence that high-frequency stimulation of the subthalamic nucleus bridles neuronal activity in the subthalamic nucleus and the substantia nigra reticulata. FASEB J. *17*, 1820–1830.

Temperli, P., Ghika, J., Villemure, J.G., Burkhard, P.R., Bogoussavsky, J., and Vingerhoets, F.J.G. (2003). How do parkinsonian signs return after discontinuation of subthalamic DBS? Neurology *60*, 78–81.

Welter, M.L., Houeto, J.L., Bonnet, A.M., Bejjani, P.B., Mesnage, V., Dormont, D., Navarro, S., Cornu, P., Agid, Y., and Pidoux, B. (2004). Effects of high-frequency stimulation on subthalamic neuronal activity in parkinsonian patients. Arch. Neurol. *61*, 89–96.

Wichmann, T., and DeLong, M.R. (1999). Oscillations in the basal ganglia. Nature *400*, 621–622.